Coastal Groundwater Flow and Associated Nutrient Transport into the Sea

Yusuke UCHIYAMA

Hasaki Oceanographical Research Station,
Port and Harbour Research Institute, Ministry of Transport
3-1-1 Nagase, Yokosuka 239-0826, Japan

ABSTRACT

A numerical model is developed to examine coastal groundwater processes in a sandy beach, including the effects of tidal fluctuations, saltwater intrusion into an aquifer, and dynamics in unsaturated layers. The simulation results indicate: 1) 'Local circulation' is clearly formed in the aquifer near the shoreline owing mainly to tidal oscillations. 2) The circulation induces a landward bending profile of salinity, wherein saline seawater is present. 3) As land-derived freshwater discharge increases, the circulation cell decreases in size and finally almost disappears. Subsequently, the model is linked with the nutrient data sampled in the aquifer of the sandy beach, Hasaki, Japan, for estimating nutrient transport into the sea. The nutrient flux via groundwater seepage is considered to have a minor component of marine nutrient budget in the surf zone; river discharge dominates at this beach.

Key Words: *groundwater, local circulation cell, numerical simulation, and nutrient flux*

1. INTRODUCTION

Groundwater flow in beaches and associated material transport plays a significant role in sediment transport mechanisms at the foreshore, coastline stability, the design of most coastal structures, and marine ecosystems of coastal flora and fauna. Since it is generally impossible to directly measure complicated velocity fields in coastal aquifers, a numerical model describing the groundwater dynamics is strongly expected to be of great advantage to the prediction of detailed groundwater flow.

During the ebb tide the beach water table may be decoupled from the ocean, resulting in the formation of a seepage face (i.e., the beach face between the exit point of the water table and the shoreline) where groundwater outcrops on the intertidal profile [e.g., *Nielsen*, 1990; *Turner*, 1993]. The groundwater flow field in the intertidal zone is important for evaluating material transport due to submarine groundwater discharge (SGWD) as shown in Figure 1 [e.g., *Johannes*, 1980]. Since unsaturated layers are attributed to the pressure potential distribution near the groundwater table, including the intertidal zone, the numerical model should be based on the Richards equation for saturated-unsaturated flow [*Richards*, 1931]. In addition, density effects induced by intrusion of saline seawater are not negligible in analyzing flow in a coastal aquifer. *Pinder and Cooper* [1970] demonstrated the movement of the saltwater front in confined coastal aquifers by using a numerical model. Their model used a steady groundwater flow equation and a time-dependant advection-dispersion equation for salinity. *Segol et al*. [1975] employed this model for a computation of steady flow in unconfined aquifers. Others incorporated Richards equation for unsteady flow [e.g., *Kohno et al*., 1983]. Although the previous works have treated transient flow related to surface recharge and drainage in coastal aquifers, unsteady flow due to the fluctuating tides and waves has not been simulated using this framework. *Li et al*. [1997a] recently presented a Boundary Element Method model solving the Laplace equation for saturated flow in an unconfined coastal aquifer. They incorporated the capillary effects derived from the approximate solution of the one-dimensional Richards equation [*Parlange and Brutsaert*, 1987] into the model and demonstrated beach water table fluctuations due to tides and waves [*Li et al*., 1997a, 1997b]. In their model, however, spatial distribution of hydraulic conductivity could not be included. Additionally, they neglected the effect of density-driven flow caused by the presence of salt water.

Coastal marine ecosystems are affected by dissolved nutrient inputs from circulating offshore water, river runoff, and groundwater seepage. The regional nutrient budget also includes atmospheric deposition, fertilizer application, wastewater treatment plant discharge, livestock waste, and decomposition of organic matter in sediment. Among these sources, the effects of groundwater on marine environments are not as well known as those of river water and offshore water. Groundwater containing inorganic nutrients can have a significant influence on coastal ecosystems, especially when nutrient concentrations are high or the relative contribution of submarine groundwater discharge (SGWD) is large. Due to nutrient leaching from surface-applied fertilizers, groundwater usually has a higher concentration of inorganic nutrients than does seawater. Therefore, even low rates of SGWD often needs to be accounted for in the nutrient budget for a coastal ecosystem [e.g., *Rölke et al.*, 1998].

Fresh groundwater flows out to the sea through a narrow seepage face as shown in Figure 1. The

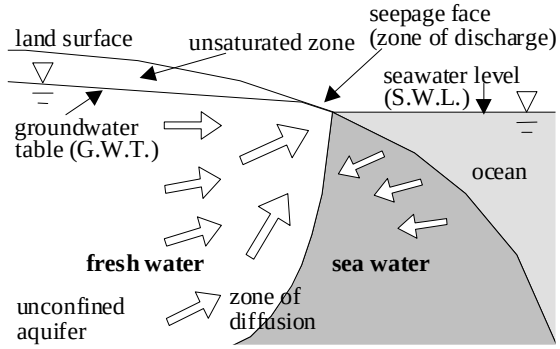

Figure 1: Conceptual illustration of submarine groundwater discharge in an unconfined coastal aquifer (e.g., *Johannes*, 1980).

velocity field in a coastal aquifer appears to be complicated by the influence of the saltwater wedge and sea-level variances. Previous studies have mostly not taken into account the spatially variable flow-field. Since it is extremely difficult to measure the flow in the aquifer directly, piezometers are often used to obtain data on the head field from which the flow patterns can be inferred [e.g., *Neilsen and Dunn*, 1998]. On the other hand, the Darcy's Law and Ghyben-Herzberg relation have been used to calculate the velocity approximately [*Raghunath*, 1982; *McLachlan and Illenberger*, 1986]. Previous estimates of SGWD have generally yielded worldwide figures in the range 0.01 to 10% of total discharge into the sea [e.g., *Church*, 1996; *Johannes*, 1980]. Nevertheless, *Moore* [1996] and *Church* [1996] inferred from ^{226}Ra measurements in coastal waters that SGWD into the South Atlantic Bight might amount to a flux equivalent to 40% of the total flow entering the sea from adjacent rivers. It is unsure whether the figure of 40% is precise, however, the uncomplicated calculations might lead to misestimates of SGWD as discussed by *Younger* [1996].

In the study reported below, a numerical model is developed to examine the coastal groundwater flows in sandy beaches, based on the Richards equation for saturated-unsaturated flow and an advection-dispersion equation for salinity. Tidal fluctuations are incorporated into the seaward boundary conditions for water levels. The advantage of the model presented here is that it can accurately simulate unsteady behavior of groundwater in unconfined coastal aquifers considering the effects of water-level fluctuations, variable-density flow, and dynamics in the unsaturated zone. The objectives of simulations are two-fold. The first is to provide some features of a local circulation, which is unique to the groundwater flow systems in sandy-beach aquifers, due to tidal variances near the shoreline. The second objective is to present an example of the model application to nutrient transport into the sea along with the field data recently collected at the sandy beach, Hasaki, Japan.

2. NUMERICAL PROCEDURE

Assuming that the aquifer studied here is isotropic, and including the variation of pressure potential due to the change of groundwater density, the Darcian flow equation can be obtained as [*Pinder and Cooper*, 1970; *Pinder and Gray*, 1977]

$$\mathbf{q} = -K(\psi)\,grad\left\{\psi - \left(\frac{\rho}{\rho_f}\right)z\right\}, \tag{1}$$

where $\boldsymbol{q} = (q_x, q_y, q_z)$ is the Darcian velocity vector, x, y, and z are respectively the longitudinal, transverse, and vertical coordinate. K is the hydraulic conductivity, ψ is the pressure potential (or matric potential in the unsaturated zone), ρ is density of mixed fluid, and ρ_f is the density of fresh water. Although the aquifer is supposed to be homogeneous in the present study, in the model K may be varied spatially and temporally in the unsaturated layers.

The Richards equation for saturated-unsaturated groundwater flow, which requires no special treatment of the groundwater table, is derived from Eq.(1) and mass conservation of pore water [*Richards*, 1931], using matrix notation.

$$\left(C_w(\psi) + \beta_0 S\right)\frac{\partial \psi}{\partial t} = \frac{\partial}{\partial x_i}\left(K(\psi)\frac{\partial \psi}{\partial x_i} - \delta_{i,3}K(\psi)\frac{\rho}{\rho_f}\right) \tag{2}$$

where i =1,2,3, x_i is the i-directional coordinate corresponding to x, y, and z. $C_w(\psi) \equiv \partial\theta/\partial\psi$ is the slope of the soil-water retention curve (or the water capacity), $\theta(\psi)$ is the volumetric water content, t is time, S is the specific storage, β_0 is a variable, and $\delta_{i,3}$ is the Kronecker δ. On the assumption that the porosity does not vary with fluctuations of the pressure potential, β_0 is expressed as

$$\beta_0 = \begin{cases} 0 & \cdots \quad unsaturated, \\ 1 & \cdots \quad saturated. \end{cases} \tag{3}$$

If the dispersion in the aquifer is assumed to be isotropic, the advection-dispersion equation governing a passive and conservative solute (e.g., salinity) is defined as Eq. (4).

$$\frac{\partial \theta C}{\partial t} + \frac{\partial}{\partial x_i}\left(\theta q_i' C\right) = \frac{\partial}{\partial x_i}\left(\theta D_{i,j}\frac{\partial C}{\partial x_j}\right), \tag{4}$$

in which j =1,2,3, and q_i' is the i-directional component of the pore water velocity vector (q_x'= q_x/θ_s, q_y'= q_y/θ_s, q_z'= q_z/θ_s, where θ_s is field-saturated volumetric water content). C is the non-dimensional

Table 1: Hydraulic parameters of the system being simulated.

S	K_s (cm/s)	ρ_f (g/cm^3)	ρ_s (g/cm^3)	θ_s	θ_r	m	α_L (cm)	α_T (cm)	ψ_0 (cmH_2O)
1.0×10^{-3}	1.331×10^{-2}	1.0	1.025	0.3759	1.0×10^{-3}	3.0	100.0	10.0	-100

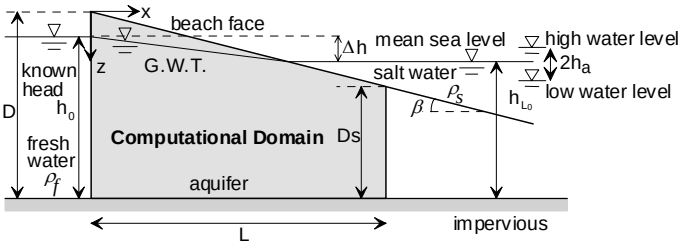

Figure 2: Schematic cross-sectional diagram of groundwater flow in an unconfined coastal aquifer for the computations. The shaded area corresponds to the computational domain. tanβ: beach slope, D, Ds: thickness of the aquifer at the landward and seaward boundaries, L: horizontal length of the computational domain, h_0: groundwater table at the landward boundary, h_{L0}: mean sea level, h_a: amplitude of the tidal fluctuations, $\Delta h = h_0 - h_{L0}$.

solute concentration (e.g., non-dimensional salinity). $D_{i,j}$ is the dispersion coefficient tensor constituting the nine components (D_{xx}, D_{xy}, D_{xz}, D_{yx}, D_{yy}, D_{yz}, D_{zx}, D_{zy}, and D_{zz}). The values of the components of $\theta D_{i,j}$ are calculated using the function proposed by *Scheidegger* [1961] and *Bear* [1972] ,

$$\theta D_{i,j} = \theta \begin{bmatrix} D_{xx} & D_{xy} & D_{xz} \\ D_{yx} & D_{yy} & D_{yz} \\ D_{zx} & D_{zy} & D_{zz} \end{bmatrix} = \alpha_T |q_i| \delta_{i,j} + (\alpha_L - \alpha_T) q_i q_j / |q_i| + \theta \nu \quad (5)$$

where q_s is the velocity magnitude (= $(q_x^2+q_y^2+q_z^2)^{1/2}$), α_L and α_T are longitudinal and transverse dispersivities, $\delta_{i,j}$ is again the Kronecker δ, and ν is the kinematic viscosity of water. The values of α_L and α_T are set to be 100.0 cm and 10.0 cm.

The relation between the non-dimensional salinity C and the density of mixed fluid ρ is

$$C = (\rho - \rho_f)/(\rho_s - \rho_f), \quad (6)$$

where ρ_s is the density of seawater. Non-dimensional concentration C, hence, is 1.0 for seawater and 0.0 for fresh water.

The hydraulic conductivity $K(\psi)$ in homogeneous and isotropic porous media is constant in the saturated zone, however, it varies in response to the change of the volumetric water content $\theta(\psi)$ in the unsaturated zone. In the present model, the relationship between $K(\psi)$ and $\theta(\psi)$ proposed by *Brooks and Corey* [1966] is employed. Ignoring hysteresis and local anisotropy, and considering the pressure head ψ as the dependent variable, they derived

$$K = K_s \{(\theta - \theta_r)/(\theta_s - \theta_r)\}^m, \quad (7)$$

where K_s is the saturated conductivity, θ_r is the residual water content, and m is a parameter which is theoretically estimated to be 3.0 by *Irmay* [1954]. The values of K_s and θ_s are experimentally obtained for the sand at Hasaki Beach: $K_s = 1.331\times10^{-2}$cm/s, $\theta_s = 0.3759$. The value of θ_r is set to be 1.0×10^{-3}. It must be emphasized that the model presented here can substantially include the effects of spatially varying hydraulic conductivity and porosity in the saturated layer whereas the sand is supposed to be homogeneous.

While various empirical functions for the retention equation exist, the one proposed by *Tani* [1982] is chosen to achieve computational robustness.

$$(\theta - \theta_r)/(\theta_s - \theta_r) = (|\psi/\psi_0| + 1)\exp(|\psi/\psi_0|), \quad (8)$$

where ψ_0 is the matric potential that gives the maximum value of the water capacity C_w.

The backward-Euler scheme was used to solve Eqs. (1) - (8). It is an iterative numerical scheme employing implicit finite-difference formulations. The spatial derivatives in equations (2) and (4) were represented by centered differences. A computational grid uniformly spaced in all directions was adopted, and the grid sizes were chosen as $\Delta x = \Delta y$ =2.0m and Δz =0.5m. The SOR (successive over relaxation) method with a relaxation parameter of ω=1.2 was applied to solve the simultaneous algebraic equations. Computational convergence was judged with tolerances of 1.0×10^{-2} for Eq.(2) and of 1.0×10^{-4} for Eq.(4). The hydraulic parameters of the system being simulated are summarized in Table 1.

In the computations, the x and y axes corresponded to the cross-shore and longshore

Table 2: Numerical configuration and a parameter for tidal forcing.

tan β	D (m)	L (m)	D_s (m)	h_a (m)
1/20	30.0	100.0	25.0	1.0

Table 3: Physical parameters for groundwater table and computational conditions.

case No.	h_0 (m)	h_{L0} (m)	Δh (m)	density	tide
1	28.5	27.5	1.0	constant	not considered
2	28.5	27.5	1.0	variable	not considered
3	28.5	27.5	1.0	constant	considered
4	28.5	27.5	1.0	variable	considered
5	28.7	27.5	1.2	variable	considered
6	28.9	27.5	1.4	variable	considered

* The acronyms in the tables are identified in the text and the caption of Figure 2.

directions, respectively. Longshore variations in ψ and C were not considered, and therefore the simulations were vertically two-dimensional. Free-flux conditions were applied above the water table. Prescribed hydrostatic head $\psi = z_0\ \rho/\rho_f$, in which z_0 is the vertical distance from the groundwater table or sea surface, and concentration (C =0.0 at the landward boundary, C =1.0 at the seaward boundary) were given as horizontal boundary conditions. Vertical boundary conditions were no-flow and no-flux conditions. The initial values of total potential and concentrations at all nodes were set to be zero; this meant that the aquifer was filled with immobile fresh water.

The model was preliminarily verified with theoretical solutions and experimental data of groundwater flows including the seepage formation at the beach face in response to the tide [see *Uchiyama*, 1999]. The results showed that the model's simulations agree with the data reasonably well.

3. COMPUTATION 1: FORMATION OF LOCAL CIRCULATION CELL

3.1 Computational Conditions

The numerical model was applied to investigate the effects of the tidal fluctuations, the variable-density flow, and the land-derived freshwater discharge on groundwater flow in an unconfined coastal aquifer. The cross section of the computational domain is schematically illustrated in Figure 2; the simulations were carried out for a portion of a sandy beach aquifer with a 1:20 uniform beach slope. The semi-diurnal tide simply represented by the sine waves was introduced here. A total of six cases were examined for various conditions as listed in Tables 2 and 3. In the cases 1 and 3 the density of groundwater was taken to be constant although its variations were incorporated in the cases 2, 4-6. The tidal variances were not considered in the cases 1 and 2 but included to simulate unsteady groundwater flows in the cases 3-6. The differences between the hydraulic heads Δh, which drove seaward groundwater flow, were changed in the cases 4-6.

In the calculations tidal amplitude h_a was initially set to be zero until the steady salt wedge was formed. Several months after the beginning of the unsteady calculations in the cases 3-6, the computed flow fields averaged over a tidal cycle were found to be unchanged; this meant the flow field could be regarded as in a state of dynamic equilibrium. Hence, the unsteady simulations were performed for ten months and then terminated. The flow fields and non-dimensional salinity distributions for the cases 3-6 presented below were obtained by averaging over the last cycle of tidal fluctuations. By introducing this procedure, residual flow patterns in the aquifer are expected to appear.

3.2 Formation of Local Circulation Due to the Tidal Fluctuations

First, the effects of the tidal fluctuations and the variable density on the groundwater flow in the coastal aquifer were examined using the model. Figures 3-(a) to (d) illustrate vector plots and streamlines of flow fields computed for the cases 1-4, respectively. Simulated non-dimensional salinity distributions for the cases 2 and 4 are displayed in Figures 4-(a) and (b).

It can be seen in Figure 3 that seaward flows driven by the hydraulic gradient imposed and upwelling flows near the shoreline appear in the aquifers for each of the cases 1-4. The phreatic surface and the bottom of the aquifer constitute streamlines, and the seabed is an equipotential line. Therefore, total potential tends to decrease toward the seabed from the upgradient area, generally attributed to this flow pattern. On the contrary, if density of fluid is set to be variable (case 2), saline seawater intrudes underneath freshwater to generate a saltwater wedge as indicated in Figure 4-(a). Since the steady saltwater-freshwater interface prevents the merging of seawater with freshwater, the seaward freshwater flow converges near the seepage face to enhance the upwelling flow. Furthermore, in the aquifer near the

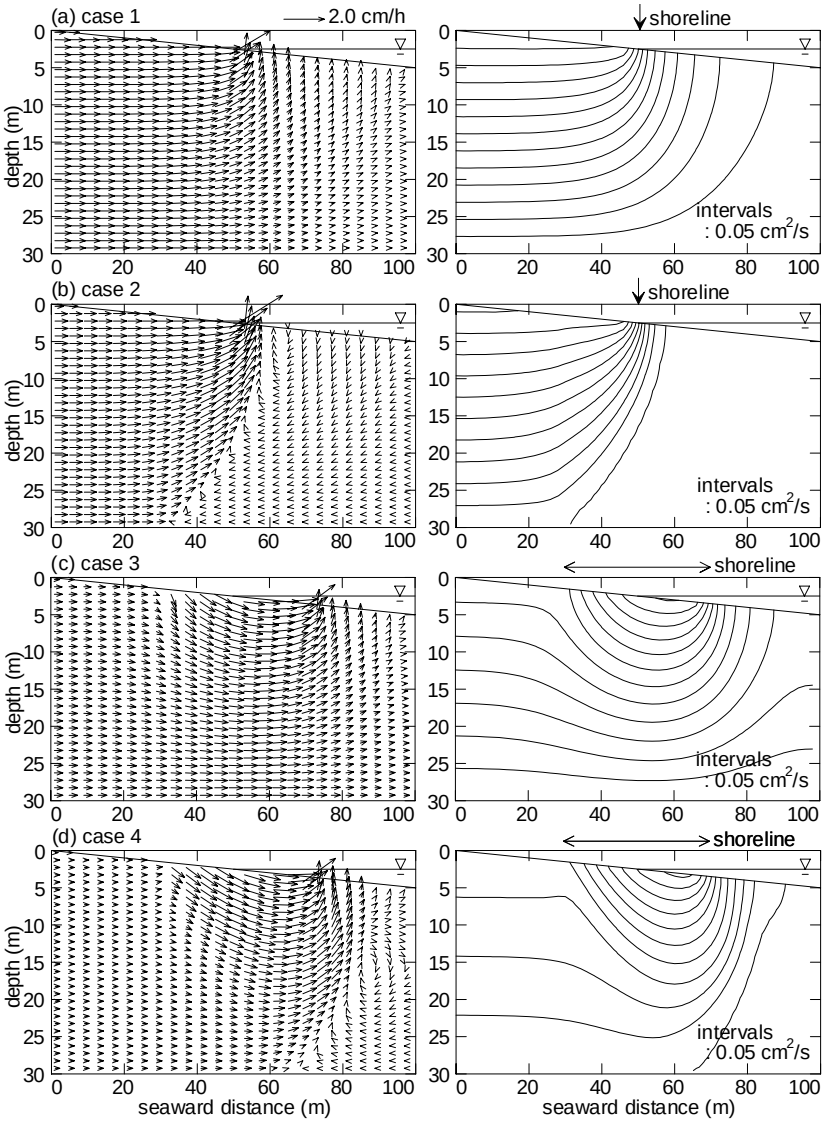

Figure 3: The vector plots and streamlines of the simulated flow fields for the cases 1 – 4 (a - d).

shoreline, the fluctuating tide induces downward flow infiltrating into the lower aquifer during floods and upward flow discharged into the sea during ebbs as shown in Figure 3-(c) and (d); local circulation is clearly formed. Yet the intruded seawater for the case 4 opposes the landward advance of the upwelling freshwater flow as well as that for the case 2, horizontal scale of the circulation cells for the cases 3 and 4 almost coincides with the traveling distance of the shoreline in response to tides. This suggests that the tidal oscillations mainly bring about the formation of the local circulation. In addition the salinity profile bending landward is attributed to this circulation, and accordingly the saltwater is observed to be present in this part (Figure 4-(b)).

3.3 Influence of Land-derived Freshwater Discharge on Circulation Size

Next, the size of the local circulation cell was examined for various values of land-derived freshwater discharge. Figure 5 shows the computed shapes of the freshwater-saltwater interfaces for the cases 4-6. It must be addressed that each of the upper portions of the interfaces approximately correspond to the sizes of the circulation cells formed in the upper layers of the aquifers. While the conditions of the tidal forcing for these three cases were the same, the difference between hydraulic heads Δh was set to gradually increase from the case 4 to case 6. As the freshwater discharge increases (i.e., from the case 4 to 6), the seaward hydraulic gradient acting on the system sufficiently upheaves the circulation cells near the shoreline, therefore, the cell decreases in size and finally almost disappears.

4. COMPUTATION 2: NUTRIENT FLUXES INTO THE SEA BY SGWD

In order to demonstrate an example of the model application to a nutrient budget in a nearshore sea, the simulation was made for estimating nutrient fluxes into the sea due to coastal groundwater flow along with the sampled

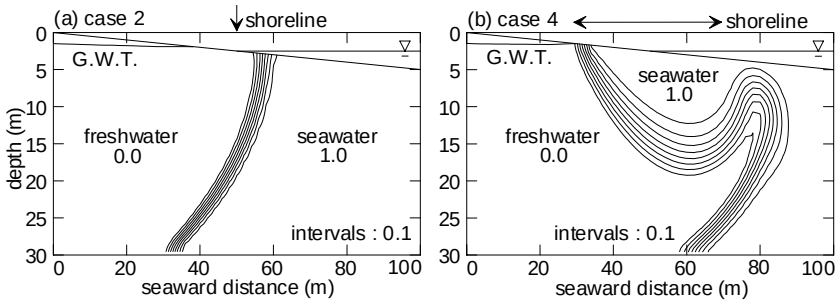

Figure 4: Simulated non-dimensional salinity distributions for the (a) case 2 and (b) case 4. The tidal fluctuations were incorporated in the case 4.

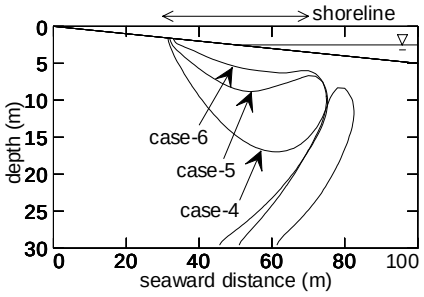

Figure 5: Shapes of the freshwater-saltwater interfaces for the cases 4-6. The land-derived freshwater discharge was set to gradually increase from the case 4 to 6.

nutrient data. In this section, a brief description of a field measurement and its results are presented, and then nutrient fluxes by groundwater and river water are calculated to discuss their influence on a marine nutrient budget.

4.1. Field Observation in Hasaki Beach

The field measurements were conducted at Hasaki Beach located along the Kashima coast, Japan, facing the Pacific Ocean (Figure 6) from August 7 to December 12, 1997. An uninterrupted sandy beach extends approximately 16 km from the Tone River mouth to the Kashima Port. Observation wells were installed near the Hasaki Oceanographical Research Station (HORS), the observatory facility of the Port and Harbor Research Institute and 12 km north of the river mouth. The Tone River is one of the longest rivers in Japan (322 km) and has the largest drainage basin (15,760 km^3). A 150-500m surf zone on the seaward side and a dune 120m from the shoreline flanks Hasaki Beach. Landward of the dune, pine trees have been planted for approximately 100m. Behind the pine-tree strip, a highly agricultural area (4-5 km wide) begins, mostly covered with paddy fields. According to the survey during drilling of the observation wells, the soil in Hasaki appears to be nearly homogeneous and highly permeable sand. The groundwater aquifer at Hasaki Beach is considered to be unconfined and to have an aquiclude approximately 30-40 m below the ground surface. These are approximately valid over monitored section based on drilling results.

The field measurements were conducted from August 7 to December 12 in 1997. A cross-section displayed in Figure 7 illustrating locations of seventeen observation wells installed at Hasaki Beach. Three of them were placed near the shoreline with D.L.+2.2 m (referred to as Sta.1) and the others (i.e., Sta.2-6) were installed landward of Sta.1. D.L. means the datum level of Hasaki Fishery Port, and is equivalent to the low water level. High water level approximately corresponds to the ground level at Sta.1. Clusters of two to five wells screened at different depths were installed at five of the six stations as shown in Figure 7. Two different depths were considered in the upgradient area and five different depths near the shoreline. The screen lengths were extended in inland wells to 8-10 m long to acquire average results for a large groundwater layer. The ground levels (G.L.), averaged groundwater table (G.W.T.), and top levels of the wells (W.L.) measured from D.L. are also displayed in Figure 7.

Samples of the groundwater in the coastal aquifer were taken on August 7 and 22, September 5 and 25, October 9 and 31 and December 12. The groundwater samples were immediately frozen and subsequently analyzed in a laboratory with a TRAACS-800 autoanalyser (Bran+Ruebbe Co.) to determine the concentrations of NO_2^-, NO_3^-+NO_2^-, NH_4^+, PO_4^{3-}, and SiO_2. In addition, water samples were collected from the Tone River mouth and from the beach shoreline. Water table elevations were also monitored every ten minutes over five months from August to December in 1997 in the observation wells of Sta.4-6 by using pressure gages (Diver, Eijkelkamp Co.). Tide levels were observed at the tip of the observatory pier of HORS. The detailed information on the field observations and interpretations of the data can be found in the citation [*Uchiyama, et al.*, 1999].

4.2. Nutrient Distributions and Groundwater Flow Field in the Aquifer

Figure 8 indicates spatially interpolated mean distributions of (a)NO_3^-, (b)NO_2^-, (c)NH_4^+, and (d) PO_4^{3-} by averaging the data obtained from August 7 to October 9. *Uchiyama, et al.* [1999] concluded from the observational results: 1) During summer,

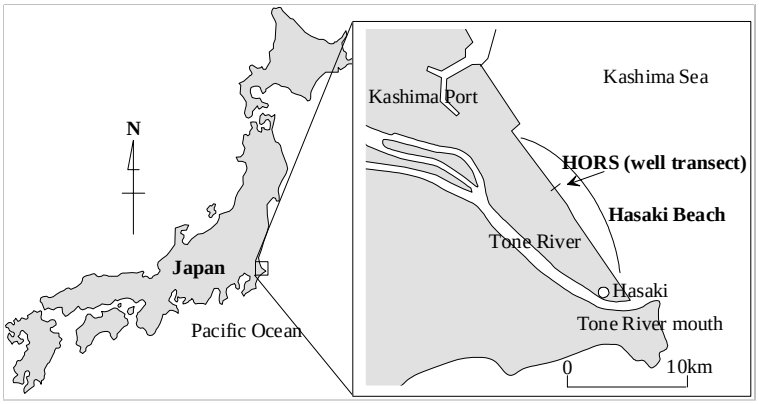

Figure 6: Location of the field measurements in Hasaki Beach, Japan.

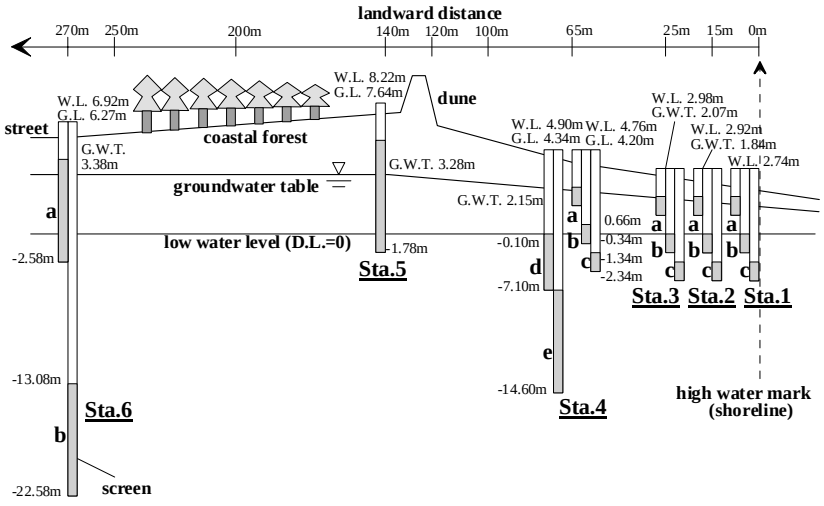

Figure 7: Location of the observation wells near HORS. Sta.1 is located at the high water mark. D.L. is the datum level of Hasaki Fishery Port, being equivalent to low water level. The ground levels (G.L.), averaged groundwater table (G.W.T.), and top levels of the wells (W.L.) measured from D.L. are also displayed.

nitrification produces high nitrate concentrations in the landward upper aquifer under aerobic conditions, while nitrite and ammonium concentrations are low. 2) The aquifer near the shoreline is a complex chemical environment in which denitrification and nitrification simultaneously or alternately occur. 3) SGWD from the upgradient area and decomposition and mineralization of organic matter from the sea supply inorganic nutrients to this part of the aquifer; those are mixed together and then transported into the sea. 4) The microbial activity related to biochemical processes in the aquifer near the foreshore zone varies seasonally as evident in the seasonal changes of the nutrient concentrations.

In order to estimate the groundwater velocity near the shoreline, fluctuation of seawater level due to tides and waves, and groundwater-table variation with precipitation should be included in the numerical simulation. Net groundwater flow may not be greatly influenced by waves, which require short time steps to simulate, and the simulation would become costly with wave included. Therefore, only the effects of variations of the groundwater table with tide and precipitation were incorporated in the simulation. The measured groundwater tables and tide levels were actually used for the landward and seaward boundary conditions.

Computations were performed for three years; the last three months corresponded to a part of the observational period, from August 1 to October 31, 1997. Figures 9 shows calculated results: (a) velocity field and (b) non-dimensional salinity distribution, both averaged over a day representative of August 22, 1997. It can be seen from the flow fields that the seeping area has the greater velocities than the interior domain, and that local circulation cells are not obviously formed. This may caused by irregularity of tidal fluctuations and larger seaward freshwater discharge. The upper part of the saltwater wedge in the aquifer was inclined toward the upgradient area as well as the computational results shown in Figure 4 and 5. The water-table fluctuations largely affect the flow and mass transport processes in the aquifer near the shoreline, where biochemical

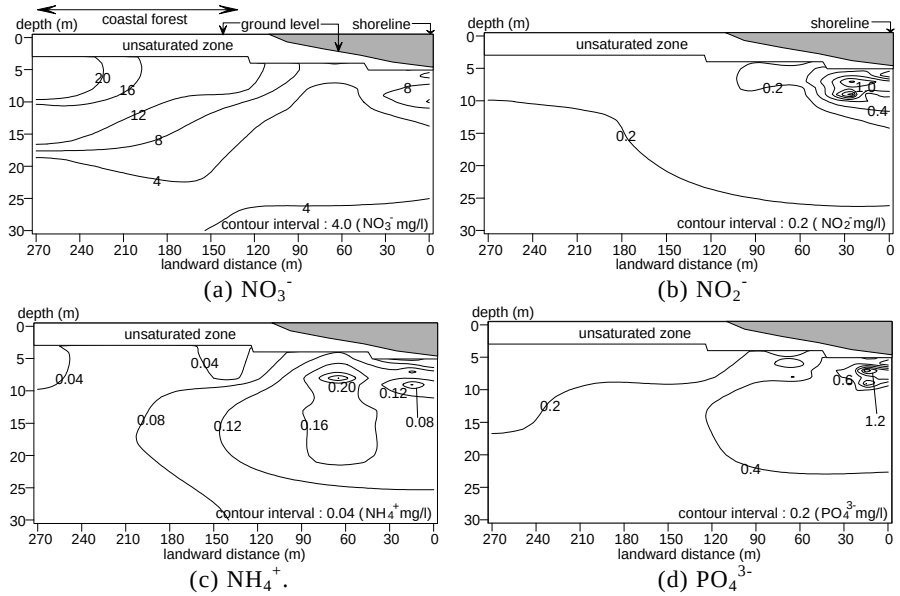

Figure 8: Spatial distributions of (a) nitrate, (b) nitrite, (c) ammonium, and (d) phospate concentration collected by *Uchiyama et al.*(1999). These illustrate their spatially interpolated mean distributions by averaging the data obtained from August 7 to October 9, 1997.

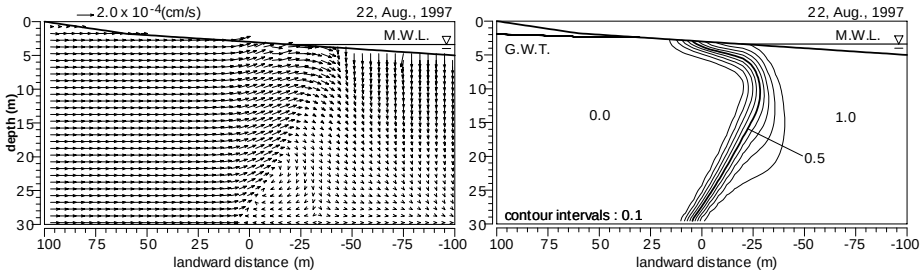

Figure 9: Computational results: spatial distribution of (a) velocity vectors, (b) non-dimensional salinity.

Table 4: Nutrient fluxes by the groundwater seeping and Tone River discharge.

	Groundwater (kg/day)	Tone River (kg/day)
NO_3^--N	54.8	22867.3
NO_2^--N	4.5	648.5
NH_4^+-N	4.7	3601.2
PO_4^{3-}-P	7.8	1349.6
SiO_2-Si	435.1	11903.9

reaction has significant importance and nutrient distribution appreciably varies with depth (Figure 8).

4.3. Nutrient Fluxes into the Sea by SGWD

In order to investigate nutrient budgets in the shallow sea, the nutrient fluxes into the sea by SGWD were examined using the computed velocity field and the measured nutrient concentrations in the aquifer near the shoreline. Table 4 lists the seaward nutrient fluxes caused by SGWD through the cross section at Sta.1 and by the Tone River discharge. The former was averaged over the whole observational period and an alongshore distance of 16.0 km was used in the calculation of SGWD. This distance corresponds to the natural uninterrupted coastline from the Tone River mouth in the south to the Kashima port in the north. For calculations of the Tone River discharge, the available data from 1993-1995 (in m^3/s) were used. In these three years the mean discharge was 212.2 m^3/s. It can be seen from Table 2 that river discharge dominates nutrient supply to the Kashima Sea; the groundwater contribution is minor. However, since not all the nutrients released from the river mouth enter the study area, the results shown in Table 4 must be carefully interpreted.

Satellite images suggest to show that the Tone River plumes drift mostly southward, and consequently less direct nutrient supply to the Kashima Sea (i.e., north of the Tone River mouth) is expected. Even though the river outflow is a major source of nutrients to the seawater in the Kashima Sea, its contribution to the shallow water environment may not be as high as that due to SGWD. On the contrary, the Tone River, which has the largest drainage basin in Japan and a proportionally large

amount of discharge, provides enormous nutrient fluxes as shown in Table 4. In a coastal area with less river influence, nutrient inputs due to SGWD may be more significant than that in the study area. Furthermore, outfalls, irrigation channels, and streams, which can be seen in the field, probably introduce nutrient-rich water directly into the nearshore sea. These nutrient supplies should be considered in analyses of nutrient budgets in future work.

5. CONCLUSION

Coastal groundwater processes in sandy beaches have been examined using a numerical model. The model includes effects of tidal fluctuations, variable density, and dynamics in unsaturated zones. The computations have been performed to provide some features of a local circulation formed in the coastal aquifers and to present an example of the model application to the nutrient transport into the sea with the nutrient data sampled at the Hasaki Beach.

The main conclusions obtained from the simulation results are as follows:

1. Local circulation cells are clearly formed in the aquifer near the shoreline owing mainly to the tidal fluctuations. The salinity profile bending landward is attributed to this circulation, and accordingly the saltwater is observed to be present in this part.
2. As the freshwater discharge increases, the circulation decreases in size and finally almost disappears.
3. The nutrient flux via groundwater seepage is considered to have a minor component of marine nutrient budget in the surf zone. The Tone River discharge dominates at the studied beach.

ACKNOWLEDGMENTS

The author gratefully acknowledges the assistance of Prof. K. Nadaoka, Dr. H. Yagi, Dr. P. Rölke (Tokyo Institute of Technology, Tokyo, Japan), and Ms. K. Adachi (National Research Institute of Fisheries Engineering, Hasaki, Japan) for their help, suggestions and critical comments.

REFERENCES

Bear, J. (1972): *Dynamics of fluids in porous media*, Dover Scientific, New York, pp.579-663.

Brooks, R.H. and Corey, A.T. (1966): Properties of porous media affecting fluid flow, *Proc. ASCE, IR*, Vol.92, pp.61-88.

Church, T.M. (1996): An underground route for the water cycle, *Nature*, No.380, pp.579-580.

Irmay, S. (1954): On the hydraulic conductivity of unsaturated soils, *Trans. AGU*, Vol.35, pp.463-467.

Johannes, R.E. (1980): The Ecological Significance of the Submarine Discharge of Groundwater, *Marine Ecol. Progr. Ser.*, Vol.3, pp.365-373.

Kohno, I., Nishigaki, M. and Tanaka, S. (1983): Finite element analysis of transient intrusion of saline water in saturated-unsaturated seepage, *Proc. of JSCE*, No.331, pp.133-141 (in Japanese).

Li, L., Barry, D.A., Parlange, J.Y. and Pattiaratchi, C.B. (1997a): Beach water table fluctuations due to wave run-up: Capillary effects, *Water Resour. Res.*, Vol.33, pp.935-945.

Li, L., Barry, D.A. and Pattiaratchi, C.B. (1997b): Numerical modeling of tide-induced beach water table fluctuations, *Coastal Eng.*, Vol.30, pp.105-123.

McLachlan, A. and Illenberger, W. (1986): Significance of Groundwater Nitrogen Input to a Beach/ Surf Zone Ecosystem, *Stygologia*, Vol.2 (4), pp.291-296.

Moore, W.S. (1996): Large groundwater inputs to coastal waters revealed by ^{226}Ra enrichments, *Nature*, No.380, pp.612-615.

Nielsen, P. (1990): Tidal dynamics of the water table in beaches, *Water Resour. Res.*, Vol.26, pp.2127-2134.

Nielsen, P. and Dunn, S.L. (1998): Manometer tubes for coastal hydrodynamics investigations, *Coastal Eng.*, Vol.35, pp.73-84.

Parlange, J.Y. and Brutsaert, W. (1987): A capillary correction for free surface flow of groundwater, *Water Resour. Res.*, Vol.20, pp.805-808.

Pinder, G. F. and Cooper, Jr. H. H. (1970): A numerical technique for calculating the transient position of the saltwater front, *Water Resour. Res.*, Vol.6, pp.875-882.

Pinder, G.F. and Gray, W. G. (1977): *Finite element simulation in surface and subsurface hydrology*, Academic Press, London, p.295.

Raghunath, H.M. (1982): *Ground Water*, Wiley Eastern Limited, pp.1-456.

Richards, L.A. (1931): Capillary conduction of liquids through porous mediums, *Physics*, Vol.1, pp.318-333.

Rölke, P., Uchiyama, Y., Adachi, K., Nadaoka, K. and Yagi, H. (1998): Submarine groundwater discharge and associated nutrient transport: a field survey in the Hasaki coast facing the Pacific Ocean, *Tech. Rep.*, No. 57, Dept. Civil Eng., Tokyo Inst. of Tech., pp.13-27.

Scheidegger, A.E. (1961): General theory of dispersion in porous media, *J. Geophys. Res.*, Vol.66, pp.3273-3278.

Segol, G., Pinder, G.F. and Gray, W.G. (1975): A Galerkin-finite element technique for calculating the transient position of the saltwater front, *Water Resour. Res.*, Vol.11, pp.347-353.

Tani, H. (1982): Characteristics of surface water rising due to vertical one-dimensional unsaturated flow, *J. of Forestry*, No.64, pp.409-418.

Turner, I.L. (1993): Water table outcropping on macro-tidal beaches: A simulation model, *Mar. Geol.*, No.115, pp.227-238.

Uchiyama, Y., Rölke, P., Adachi, K., Nadaoka, K. and Yagi, H. (2000): Submarine groundwater discharge into the sea and associated nutrient transport in a sandy beach, *Water Resour. Res.* (in print).

Uchiyama, Y. (1999): Numerical analysis on groundwater flow in sandy beaches considering tidal fluctuation and density distribution, *Rep. Port and Harbour Res. Inst.*, Vol.38, No.2, pp.4-29. (in Japanese)

Younger, P.L. (1996): Submarine groundwater discharge, *Nature*, No.382, pp.121-122.

This manuscript was presented in *2nd UJNR/CEST Panel*, Charleston, Mary Land, Oct., 1999, sponsored by NOAA NOS.

Dr. Yusuke Uchiyama: HORS, PHRI, Sudahama, Hasaki 314-0253, Japan (at present)
Phone: +81-479-461852, Fax: +81-479-460679, E-mail: uchiyama@ipc.phri.go.jp